




Coordinated plasticity maintains hydraulic safety in sunflower leaves

Amanda A. Cardoso^{1,2,3}  | Timothy J. Brodribb¹  | Christopher J. Lucani¹ | Fábio M. DaMatta² | Scott A.M. McAdam³ 

¹School of Biological Sciences, University of Tasmania, Hobart, TAS 7001, Australia

²Departamento de Biologia Vegetal, Universidade Federal de Viçosa, Viçosa 36570-900MG, Brazil

³Purdue Center for Plant Biology, Department of Botany and Plant Pathology, Purdue University, West Lafayette, IN 47907, USA

Correspondence

T. J. Brodribb, School of Biological Sciences, Private Bag 55, University of Tasmania, Hobart, TAS 7001, Australia.
Email: timothyb@utas.edu.au

Funding information

Australian Research Council, Grant/Award Numbers: DE140100946 and DP140100666; FAPEMIG, Grant/Award Number: BDS-00404-15

Abstract

The xylem cavitation threshold water potential establishes a hydraulic limit on the ability of woody species to survive in water-limiting environments, but herbs may be more plastic in terms of their ability to adapt to drying conditions. Here, we examined the capacity of sunflower (*Helianthus annuus* L.) leaves to adapt to reduced water availability by modifying the sensitivity of xylem and stomata to soil water deficit. We found that sunflower plants grown under water-limited conditions significantly adjusted leaf osmotic potential, which was linked to a prolongation of stomatal opening as soil dried and a reduced sensitivity of photosynthesis to water-stress-induced damage. At the same time, the vulnerability of midrib xylem to water-stress-induced cavitation was observed to be highly responsive to growth conditions, with water-limited plants producing conduits with thicker cell walls which were more resistant to xylem cavitation. Coordinated plasticity in osmotic potential and xylem vulnerability enabled water-limited sunflowers to safely extract water from the soil, while protecting leaf xylem against embolism. High plasticity in sunflower xylem contrasts with data from woody plants and may suggest an alternative strategy in herbs.

KEYWORDS

cavitation, herbaceous species, osmotic adjustment, stomatal movement, xylem vulnerability

1 | INTRODUCTION

Plant water transport through xylem cells is mostly driven by tension gradients generated at air–water interfaces within leaves (Dixon & Joly, 1895). Transporting water under tension is free of metabolic costs; however, the instability of water at high tension results in an inevitable consequence: a vulnerability of the xylem to cavitation (Sperry & Tyree, 1988). When plants are exposed to drying soils or high evaporative demands, tensions generated in the xylem vasculature can exceed a limit (i.e., “air-seeding” threshold) where an air bubble is pulled into the conduit lumen, where it rapidly expands to form an air cavity that blocks the xylem (i.e., cavitation; Tyree & Sperry, 1989). Drought-induced cavitation reduces the plant hydraulic conductance, including leaf hydraulic conductance (K_{leaf} ; Brodribb et al., 2016), negatively impacting photosynthetic gas exchange (Brodribb, Feild, & Jordan, 2007; Sack & Holbrook, 2006). The xylem

vulnerability to cavitation emerges therefore as a primary constraint on vascular plant-function (Tyree & Sperry, 1989).

Xylem vulnerability in herbs has been traditionally difficult to measure due to technical limitations (Lens et al., 2016), but the available data suggest that herbs are highly sensitive to cavitation (Li, Sperry, & Shao, 2009; Saha, Holbrook, Montti, Goldstein, & Cardinot, 2009; Stiller & Sperry, 2002). Recent studies showed that the entire xylem system of tomato plants, including roots, stems and leaves, experienced approximately 40% of cavitation at the very mild water potential of approximately -1.5 MPa (Skelton, Brodribb, & Choat, 2017). Given the tendency for high xylem vulnerability to be associated with low construction cost and high transport efficiency (Hacke, Sperry, Wheeler, & Castro, 2006; Larter et al., 2015), the expression of vulnerable xylem in herbs certainly accords with the general impression of herbaceousness as occupying the “fast” end of the plant economics spectrum (Reich, 2014). Yet at the same time, high

vulnerability to cavitation poses questions about the functionality of herbs during water stress. Two scenarios threaten to cause cavitation and loss of productivity in vulnerable herbaceous plants; the first is the possibility of cavitation caused by strong transpiration in well-watered plants, and the second is cavitation produced by soil drying. Many herbs have very high maximum stomatal conductances (g_s), potentially exposing them to massive rates of transpiration, which could drive leaf water potentials (Ψ_{leaf}) sufficiently negative to induce cavitation (Oren et al., 1999; Sperry, 2000). Stomatal closure in response to declining Ψ_{leaf} has been observed to arrest leaf dehydration before xylem cavitation occurs (Brodrribb & McAdam, 2017; Cochard, Coll, Le Roux, & Améglio, 2002; Martin-StPaul, Delzon, & Cochard, 2017). Yet the possibility of wrong-way stomatal responses (Buckley, 2005) caused by very rapid changes in transpiration could allow transient water potential excursions into the danger zone for cavitation. However, the danger of cavitation induced by excessive transpiration in wet soil may not be especially problematic for herbaceous plants because xylem should refill either by capillarity or by root pressure if plants are allowed to equilibrate with wet soil overnight (Gleason et al., 2017).

Cavitation caused by drying soil poses a potentially more significant threat to herbs with highly vulnerable xylem because cavitation-induced embolisms are unlikely to be repairable until soils return to full hydration and atmospheric humidity approaches 100%. Thus, herbs with highly vulnerable xylem appear to be precariously exposed to changes in soil water content that could cause damage or death. Even if stomatal closure delays the dehydration of the plant body, species with highly vulnerable xylem would be incapable of extracting water from drying soil, without risking xylem failure (Choat et al., 2012). This means stomata in water-limited herbs are forced to remain closed, and plants are unable to take up CO_2 for photosynthesis. These potential costs must be balanced by the likely benefits of producing vulnerable xylem, such as reduced construction costs or improved efficiency. Quantifying these risks and benefits is essential in order to understand the ecology of herbaceousness.

Here, we focus on the risk component associated with constructing highly vulnerable xylem. Of particular interest for herbaceous species living very close to the cavitation limits of their xylem is whether the potential exists for plastic modification of xylem vulnerability under conditions of water limitation. It is known that herbaceous species are often highly plastic in terms of leaf osmotic adjustment under water limitation, which extends the water potential range of stomatal opening (Turner & Jones, 1980). However, such adjustment would appear to expose the xylem to heightened risk of cavitation unless xylem vulnerability could also be shifted to accommodate lower water potentials. Such plasticity could greatly extend the tolerance of otherwise sensitive plants to more negative soil water potentials. The possibility of xylem acclimation during exposure to reduced water availability has been identified as a potentially important issue in woody plants (Anderegg, 2014), yet there is little information about plasticity in herbs, where the threat of cavitation is likely to be most profound. Sunflower (*Helianthus annuus* L.) makes an ideal subject for examining the impact of water stress on hydraulic vulnerability because this species is known to exhibit plasticity in stomatal response to water potential and leaf turgor in response to changes in growth conditions (Tardieu, Lafarge, & Simonneau, 1996).

In order to understand whether sunflower plants are able to modify their hydraulic system to accommodate drier growth conditions, we measured the leaf xylem vulnerability and stomatal responsiveness to leaf-air vapour pressure deficit (VPD) of plants grown under both well-watered and water-limited soil. We hypothesised that sunflower plants grown under water-limited soils would exhibit leaf xylem that was less vulnerable to cavitation, and leaves less vulnerable to photosynthetic damage. We further hypothesised that a coordinated shift of osmotic potential and xylem vulnerability in water-limited plants would play a critical role in prolonging leaf gas exchange while preventing extensive leaf xylem cavitation and declines in whole plant hydraulic conductance (K_{plant}) under high VPD.

2 | MATERIALS AND METHODS

2.1 | Plant material and growth conditions

Seeds of an individual *H. annuus* cv. Yellow Empress (*Asteraceae*) were germinated in approximately 3-L plastic pots containing potting mix and watered daily to full capacity until seedlings were approximately 3-weeks old. Six of the healthiest plants were divided into two random groups of three plants each, which were next grown under either well-watered or water-limited conditions for another 5 weeks. Well-watered plants were watered daily in the morning to full capacity (pre-dawn leaf water potential [Ψ_{predawn}] > -0.20 MPa; Figure 1) and kept in a glasshouse regulated at 16 hr/day at 25°C/15°C/day/night temperatures, VPD at approximately 1.0 kPa during the day, and natural light (maximum photosynthetic photon flux density [PPFD] of approximately 1,500 $\mu\text{mol}\cdot\text{m}^{-2}\cdot\text{s}^{-1}$). Water-limited plants were watered three times per week in the morning to full capacity (-0.50 MPa > Ψ_{predawn} > -1.36 MPa), resulting in a clear wilting recovery cycle (Figure 1). They were kept outside the glasshouse during summer (from December 2016 to January 2017) under a natural approximately 16 hr/day at approximately 23°C/13°C/day/night temperatures, VPD at 1.45 ± 0.7 kPa during the day, and natural light (maximum PPFD of approximately 1,800 $\mu\text{mol}\cdot\text{m}^{-2}\cdot\text{s}^{-1}$). At the end of the total 8 weeks, both well-watered and water-limited plants were approximately 100–120 cm tall, and each plant had approximately 20 leaves.

2.2 | Physiological and anatomical traits

All measurements were carried out using fully expanded leaves developed entirely during the watering treatment period. Leaves from three individuals per treatment were sampled for each measurement.

The Ψ_{predawn} and midday leaf water potential (Ψ_{midday}) were determined for well-watered and water-limited plants over the course of the week during the watering treatment period. Leaves were sampled before sunrise (0600h) and at approximately 1200h, wrapped in damp paper towel, bagged, and immediately measured using a Scholander pressure chamber (615D, PMS Instrument Company, Albany, USA).

Leaf turgor loss point (Ψ_{tlp}), leaf osmotic potential at full turgor (Ψ_s), and leaf capacitance (C_{leaf}) were determined on each of the three well-watered and water-limited plants using pressure-volume analysis

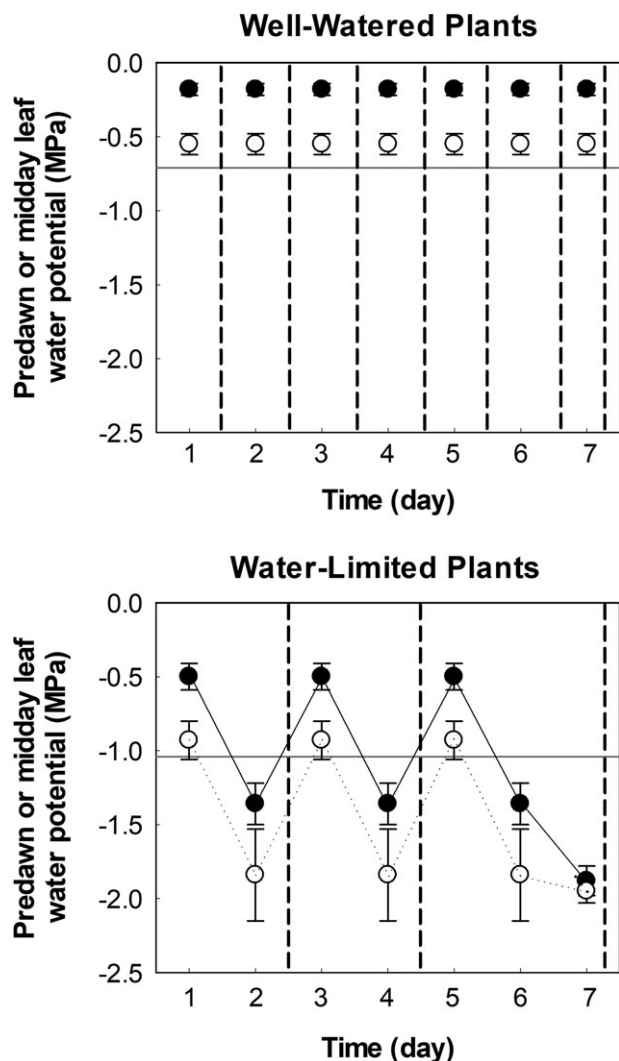


FIGURE 1 Mean predawn (black circles) and midday (white circles) leaf water potentials over the course of a week observed in *Helianthus annuus* plants ($n = 3$, \pm SD) grown under well-watered and water-limited conditions. Dashed vertical lines indicate when plants were watered. Solid horizontal line indicates the mean leaf turgor loss point

(Tyree & Hammel, 1972). Fully expanded leaves for each growth condition were cut under water and rehydrated overnight until Ψ_{leaf} was > -0.1 MPa. Leaf mass and Ψ_{leaf} were measured over time during slow desiccation on the bench until Ψ_{leaf} stopped falling. Relative water content was plotted against Ψ_{leaf}^{-1} as per Tyree and Hammel (1972). The Ψ_{tip} was determined by the inflection point between the pre-turgor loss and post-turgor loss portions of the curve. The Ψ_s was obtained by extrapolating the linear relationship of the post-turgor loss portion of the curve to 100% relative water content. Finally, the C_{leaf} was calculated in terms of relative water content from the linear slope of the plot, and normalized by leaf area.

Anatomical traits were measured from two leaves of each replicate plant using visibly undamaged leaves were collected from the third to fifth node from the distal end of the stem. For paradermal analysis, fresh leaves were divided vertically into two equal parts, and three sections of approximately 100 mm^2 (i.e., near the leaf base, in the central region, and near the tip) were taken along one of the sides. The sections were cleared using commercial bleach, rinsed,

stained with 1% toluidine blue and mounted on microscope slides in phenol glycerine jelly. Three fields of view (FOV) per section were photographed using a camera (Digital Sight DS-L1, Nikon, Melville, USA) mounted on a microscope (DM 1000, Leica, Nussloch, Germany), and the images were used to quantify vein density (D_v) and stomatal density (D_s) using the ImageJ software (National Institute of Health, New York, USA). The D_v was measured in one FOV per section at $\times 4$ magnification (FOV area 3.47 mm^2), and D_s was measured in one FOV per section at $\times 20$ magnification (FOV area 0.14 mm^2) on both sides of the leaves. For cross sections, fresh leaves were cut at approximately one-third position from the top to the bottom using a freeze-microtome (BFS-3MP, Physitemp Instruments, Clifton, USA). The sections were stained with 1% toluidine blue, and mounted in phenol glycerine jelly. Three FOVs per section were photographed, and the images were used to quantify leaf thickness (T_{leaf}), hydraulically weighted vessel diameter (D_h) and the xylem cell wall thickness (t) and lumen breadth (b) ratio $[(t/b)^3]$; a theoretical predictor of vulnerability to cell collapse; Brodribb & Holbrook, 2005]. The T_{leaf} was measured in two FOVs per section at $\times 10$ magnification, and D_h , t and b were measured in one FOV per section at $\times 40$ magnification. Both t and b were measured for all xylem conduits in the midrib; for each conduit b was calculated as the average of the maximum and minimum diameters of each lumen and t was calculated as the average of three random measurements of cell wall thickness. The D_h was calculated for each leaf using the equation (Kolb & Sperry, 1999):

$$D_h = \sum b^5 / \sum b^4 \quad (1)$$

The cell wall thickness values used for $(t/b)^3$ calculation was obtained as the value consistent with the D_h using the linear relationship between t and b for each leaf (Blackman, Brodribb, & Jordan, 2010).

2.3 | Maximum leaf hydraulic conductance

K_{leaf} was determined in plants grown under both well-watered and water-limited conditions. All individual were watered and bagged overnight, and K_{leaf} was assessed from 800 h to 1000 h by the evaporative flux method (Brodribb & Holbrook, 2006; Sack, Melcher, Zwieniecki, & Holbrook, 2002) using a flowmeter. During the morning, the leaves were acclimated to high humidity (bagged with wet paper) for approximately 30 min to ensure high g_s . Leaves were then cut under water and immediately connected to the flowmeter. PPF of $c. 600 \mu\text{mol m}^{-2} \text{ s}^{-1}$ and a constant stream of warm air were applied to the leaves (leaf temperature ranged from 27 to 32°C) allowing high rates of transpiration, and consequent high rates of flow. After flow reached a maximum steady-state for $c. 5$ min, Ψ_{leaf} was immediately measured using a Scholander pressure chamber. Calculation of K_{leaf} was made using the equation:

$$K_{\text{leaf}} = F / \Psi_{\text{leaf}}, \quad (2)$$

where F is the water flow into the leaf at steady-state condition. Values were normalized to leaf area and the viscosity of water at 20°C (Korson, Drost-Hansen, & Millero, 1969).

2.4 | Vapour pressure deficit transitions

The three individual well-watered and water-limited plants were measured in a custom built growth chamber designed to allow very rapid transitions between low and high VPD. Prior to measuring, each individual plant was watered and acclimated overnight in the chamber under dark and low VPD conditions [0.75 ± 0.2 kPa ($30 \pm 0.1^\circ\text{C}$ and $82 \pm 6\%$ relative humidity)]. The following day, lights were turned on ($300 \mu\text{mol m}^{-2} \text{s}^{-1}$ at the leaf surface) and, after 90 minutes, leaf gas exchange and Ψ_{leaf} were measured under this low VPD condition. Each plant was then transferred to an adjacent chamber under a high VPD condition [3.25 ± 0.3 kPa ($30 \pm 0.1^\circ\text{C}$ and $23 \pm 7\%$ relative humidity)] for 60 min. Relative humidity was controlled by a condensing dehumidifier (SeccoUltra 00563, Olimpia-Splendid, Gualtieri, Italy). Temperature and relative humidity were monitored every 30 s during the entire experimental period using a humidity probe (HMP45AC, Vaisala, Helsinki, Finland) and a temperature thermocouple; both connected to a data logger (CR800, Campbell Scientific, Logan, USA).

One leaf per plant was selected for instantaneous g_s measurements throughout the VPD experiment, which were performed using a portable photosynthesis system (GFS-3000, Heinz Walz, Effeltrich, Germany). Gas exchange measurements were performed under steady-state low VPD, then at 10, 20, 40 and 60 min after the step increase in VPD. Conditions in the cuvette were controlled at temperature of 30°C , $390 \mu\text{mol CO}_2 \text{ mol}^{-1}$ air, PPFD of $1,000 \mu\text{mol m}^{-2} \text{s}^{-1}$ at the leaf surface and the VPD was maintained as close as possible to the ambient chamber VPD. Maximum transient transpiration rate (E) was calculated using g_s (obtained from the gas exchange measurements) and VPD (obtained from the relative humidity of the chamber and leaf temperature measured with a thermocouple). One leaf per plant was sampled for Ψ_{leaf} at steady-state initial low VPD, at 05 and 60 min after the step increase in VPD. Leaves were collected, wrapped in wet paper towel, bagged, and placed in a humid box for Ψ_{leaf} assessment using a Scholander pressure chamber. Steady-state K_{plant} was further calculated under steady-state initial low VPD and high VPD (60 min after the VPD transition). Calculation of K_{plant} to the target leaf was made using the equation:

$$K_{\text{plant}} = E/\Psi_{\text{leaf}}, \quad (3)$$

where E (calculated from g_s and VPD) and Ψ_{leaf} under steady-state low and high VPD were used. Soil water potential in watered pots was assumed to be close to zero, as all plants, including the water-limited ones, were watered in the night before and acclimated overnight under dark and low VPD conditions until the beginning of the experiment.

To understand the hydraulic dynamics during a rapid VPD transition, E , g_s , and Ψ_{leaf} were modelled during VPD transitions under the theoretical condition of no stomatal closure and constant g_s . Maximum E (E_{max}) was calculated using the maximum g_s (i.e., obtained under steady-state initial low VPD) and values of VPD. The dynamic drop in Ψ_{leaf} was modelled assuming leaf dehydration equivalent to the charging of a capacitor through a resistor (Brodrribb & Holbrook, 2003):

$$\Psi_{\text{leaf},i+1} = \Psi_{\text{leaf},i} - \left[\Psi_{\text{min}} - \left(\Psi_{\text{min}} \times e^{-\frac{t \times K_{\text{plant}}}{C_{\text{leaf}}}} \right) \right], \quad (4)$$

where $\Psi_{\text{leaf},i}$ (MPa) is the steady-state Ψ_{leaf} under low VPD; Ψ_{min} (MPa) is the minimum Ψ_{leaf} that would be reached at steady-state conditions under high VPD, considering E_{max} ($\text{mmol m}^{-2} \text{s}^{-1}$) and K_{plant} ($\text{mmol m}^{-2} \text{s}^{-1} \cdot \text{MPa}^{-1}$); t is the time interval (s); and C_{leaf} unit was $\text{mmol m}^{-2} \text{MPa}^{-1}$. The $\Psi_{\text{leaf},i}$ was measured under low VPD during the VPD transitions using a Scholander pressure chamber; K_{plant} was obtained under high VPD during the VPD transitions; C_{leaf} was obtained using PV curve; E_{max} was calculated as $E_{\text{max}} = \text{maximum } g_s \times \text{high VPD}$; and finally, Ψ_{min} calculated as $\Psi_{\text{min}} = E_{\text{max}}/K_{\text{plant}}$.

2.5 | Optical vulnerability technique and leaf injury monitoring

Finally, each of the three replicate plants in well-watered and water-limited treatments were subjected to a lethal drying experiment to determine the vulnerability of xylem and the photosynthetic systems to damage. Prior to measurements, all plants were watered and bagged overnight. In the next morning, plants were carefully removed from pots to enhance the rate of soil drying. One leaf was placed under a stereomicroscope (M205A, Leica Microsystems, Heerbrugg, Switzerland) to record the development of cavitation in the leaf midrib, while the remaining leaves of the plant were fully covered using a thick black fabric to allow whole plant equilibration. The water potential was measured at 20-min intervals using a psychrometer attached to the stem. The water potential was also confirmed with twice-daily measurements obtained by using a Scholander pressure chamber. Images of the midrib were taken every 3 min using a camera mounted on the microscope. Images were analysed by quantifying differences in light transmission through the midrib between captured images using an image subtraction method in ImageJ (for details, see Brodrribb et al., 2016 and www.opensourceov.org). To analyse the relationship between plant water status and cavitation-induced air embolism formation, a linear regression was fitted between the drying time and water potential measurements and used to determine the water potential at the time of each image capture. These values were then plotted against total embolism area for each image to produce an optical vulnerability (OV) curve. The water potentials at 12%, 50%, and 88% of maximum cavitation in the leaf midrib (P_{12} , P_{50} , and P_{88}) were calculated based on this vulnerability curve. Each vulnerability curve was measured during approximately 72 hr, and for all individuals, the last midrib cavitation occurred at approximately 48 hr after the commencement of drying. The final 24 hr were used to ensure no more cavitation events and to finish collecting fluorescence data. A previous experiment was performed measuring K_{leaf} from well-watered and water-limited plants to confirm that water-limited plants were capable of refilling during the night, confirming that there was minimal embolism present in water-limited leaves prior to the beginning of OV measurements (for further details, see the "maximum leaf hydraulic conductance" section).

The maximum quantum efficiency of photosystem II (F_v/F_m) is a well-known parameter typically used as an index of photosynthetic potential and injury in leaves (Guadagno et al., 2017). Here, we assessed F_v/F_m in the same plants used for the OV method over the desiccation course as a proxy for leaf damage. Leaf samples were taken randomly approximately four times per day, dark-adapted for

30 min, and F_v/F_m was assessed using a portable chlorophyll fluorometer (PAM-2000, Heinz Walz, Effeltrich, Germany). Leaf tissues were illuminated with a weak modulated laser measuring beam to obtain the initial fluorescence (F_0) and then a saturating white light pulse was applied to ensure maximum fluorescence emissions (F_m), from which F_v/F_m was calculated:

$$F_v/F_m = [(F_m - F_0)/F_m]. \quad (5)$$

The dynamic changes in F_v/F_m were then presented in response to Ψ_{leaf} .

2.6 | Statistical analysis

Student's *t* tests ($n = 3$) were performed to test differences between well-watered and water-limited plants regarding the parameters Ψ_{tip} , Ψ_s , P_{50} , K_{leaf} , C_{leaf} , D_v , D_s , T_{leaf} , D_h , and $(t/b)^3$.

3 | RESULTS

3.1 | Comparative physiology and anatomy of well-watered and water-limited plants

The Ψ_{predwan} of well-watered plants was higher than approximately -0.20 MPa during the entire experimental period, whereas Ψ_{predwan} of water-limited plants ranged from -0.50 to -1.36 MPa between watering events resulting in a clear wilting-recovery cycle (Figure 1). Such water shortage during growth induced osmotic adjustments, as evidenced by significant changes in Ψ_s and Ψ_{tip} in water-limited plants to a lower Ψ_{leaf} compared with well-watered plants (Table 1).

TABLE 1 Mean values ($n = 3$, \pm SE) for leaf water potential at turgor loss point (Ψ_{tip} ; -MPa), leaf osmotic potential at full turgor (Ψ_s ; -MPa), water potential at 50% cumulative embolism (P_{50} ; -MPa), maximum leaf hydraulic conductance (K_{leaf} ; $\text{mmol}\cdot\text{m}^{-2}\cdot\text{s}^{-1}\cdot\text{MPa}^{-1}$), leaf capacitance (C_{leaf} ; $\text{mmol}\cdot\text{m}^{-2}\cdot\text{MPa}^{-1}$), vein density (D_v ; $\text{mm}\cdot\text{mm}^{-2}$), stomatal density (D_s ; mm^{-2}) on the lower epidermis, leaf thickness (T_{leaf} ; mm), hydraulically weighted vessel diameter (D_h ; $\times 10^2$), and xylem cell wall thickness (t ; mm) and lumen breadth (b ; mm) ratio ($(t/b)^3 \times 10^3$) in *Helianthus annuus* plants grown under either well-watered or water-limited conditions

Traits	Well-watered	Water-limited
Ψ_{tip}	0.71 ± 0.03	$1.04 \pm 0.02^{**}$
Ψ_s	0.60 ± 0.04	$0.79 \pm 0.04^*$
P_{50}	1.15 ± 0.07	$1.74 \pm 0.04^{**}$
K_{leaf}	11.88 ± 1.14	$11.05 \pm 0.16^{\text{ns}}$
C_{leaf}	3064 ± 102	$3417 \pm 211^{\text{ns}}$
D_v	11.31 ± 0.54	$11.58 \pm 0.17^{\text{ns}}$
D_s	286 ± 15	$320 \pm 30^{\text{ns}}$
T_{leaf}	0.233 ± 0.01	$0.254 \pm 0.01^{\text{ns}}$
D_h	2.32 ± 0.17	$2.18 \pm 0.08^{\text{ns}}$
$(t/b)^3$	1.10 ± 0.29	$4.03 \pm 0.33^{**}$

Note. Asterisks indicate significant changes in each trait (Student's *t* test) between growth conditions. ns = not significant.

* $p < .05$;

** $p < .01$.

When plants were exposed to acute soil drying, cavitation was clearly visualized in the sunflower midrib (Figure 2) with large numbers of events accumulating in a sigmoidal fashion as plants dried. The resultant midrib vulnerability curves were very different for plants grown under the two watering treatments (Figure 3). Plants grown under water-limited conditions displayed a significantly higher resistance to cavitation ($P_{50} = -1.74 \pm 0.04$ MPa) than their well-watered counterparts ($P_{50} = -1.15 \pm 0.07$ MPa; Table 1; Figure 3a). A similar pattern was observed regarding P_{12} and P_{88} , that is, -1.42 and -2.05 MPa for water-limited plants, respectively; and -1.06 and -1.24 MPa for well-watered plants, respectively. The steep slope of the vulnerability curves meant that there was no overlap in the vulnerability curves produced by leaves from the different treatments.

Strong coordination between the shift in osmotic potential and xylem vulnerability was evident in terms of a significant correlation between P_{50} and Ψ_s ($r = 0.96$; $p < .05$; Figure 4). In association with changes in P_{50} and Ψ_s in water limited plants, the water potential threshold triggering a decline in maximum quantum yield of photosystem II (F_v/F_m) also shifted to a more negative water potential in water-limited plants ($F_v/F_m < 0.75$ at -2.23 ± 0.06 MPa) than well-watered plants ($F_v/F_m < 0.75$ at -1.63 ± 0.17 MPa; Figure 3b).

Increases in resistance to cavitation in plants grown under water-limited conditions were accompanied by a higher $(t/b)^3$ ratio, driven by significant differences in the cell wall thickness rather than decreases in D_h (Table 1). Other morphophysiological traits related to hydraulic efficiency (e.g., maximum K_{leaf} , D_v , D_s , T_{leaf} and D_h) were not significantly different in plants grown under both conditions (Table 1).

3.2 | VPD responses of stomata

When sunflower plants grown under well-watered conditions were transferred from low to high VPD conditions, within the first 5 min,

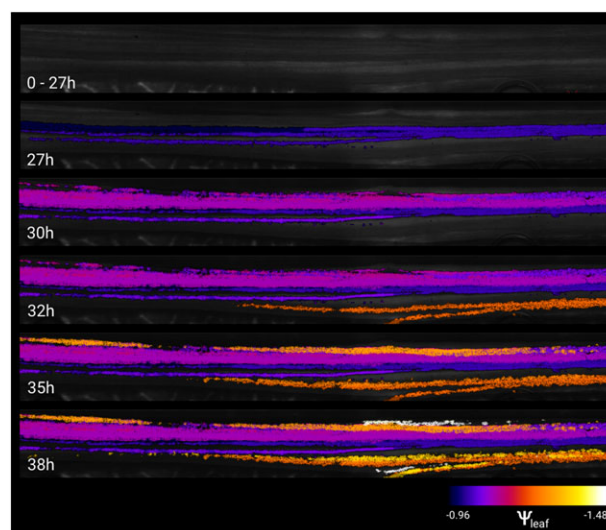


FIGURE 2 A spatio-temporal map showing the progression of cavitation events in the leaf midrib recorded in *Helianthus annuus* plants grown under well-watered conditions during the desiccation. The colour scale shows the leaf water potential (Ψ_{leaf} ; MPa) at which different cavitation events occurred. Time ranges after excision are shown in each panel

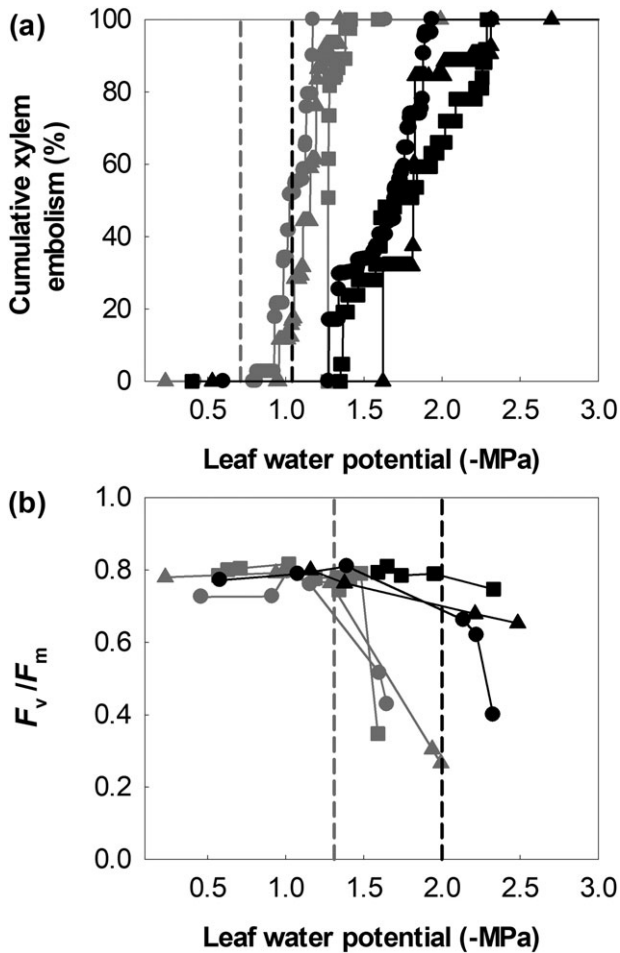


FIGURE 3 (a) Comparison of the percentage cumulative total embolism in the leaf midrib recorded during drying between *Helianthus annuus* plants grown under both well-watered (grey symbols) and water-limited (black symbols) conditions. The different symbols indicate individual leaves from different plants. The dashed vertical lines indicate the mean leaf turgor loss points for plants grown under either well-watered (grey lines) or water-limited (black lines) conditions. (b) Comparison of maximum quantum yield (F_v/F_m) recorded during drying between *H. annuus* plants grown under both well-watered (grey symbols) and water-limited (black symbols) conditions. The different symbols indicate individual leaves. The dashed vertical lines show leaf water potentials at 100% loss of xylem function in the leaf midrib for plants grown under either well-watered (grey lines) or water-limited (black lines) conditions

Ψ_{leaf} fell close to the Ψ_{tlp} , from -0.30 ± 0.02 to -0.64 ± 0.05 MPa (Figure 5b). This decline was driven by a dramatic initial increase in the transpiration rate from 3.8 ± 0.2 to 17.3 ± 0.8 $\text{mmol}\cdot\text{m}^{-2}\cdot\text{s}^{-1}$ (and even higher considering no stomatal closure immediately after the VPD transition; Figure 5a). Afterwards, g_s was shown to gradually decrease from 0.74 ± 0.1 to 0.14 ± 0.1 $\text{mol}\cdot\text{m}^{-2}\cdot\text{s}^{-1}$ (Figure 5c), resulting in a final diminished E (Figure 5a) and increased Ψ_{leaf} (Figure 5b). Modelled data indicated that without stomatal closure under high VPD, pronounced declines in Ψ_{leaf} driven by exceedingly high rates of E would lead cavitation in the leaf midrib over a very short timeframe (Figure 5b). However, no consistent dynamic was observed for K_{plant} during the VPD transitions. Although one single individual showed a decline in K_{plant} when transferred to the high VPD condition, the other two maintained similar or even higher K_{plant}

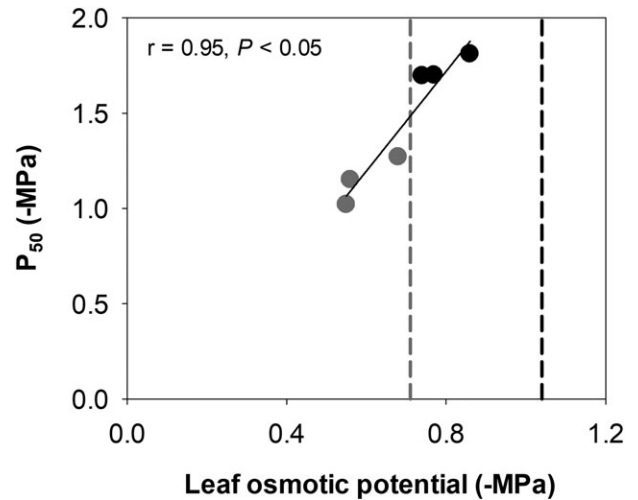


FIGURE 4 Correlation between water potential at 50% cumulative embolism in the leaf midrib (P_{50}) and leaf osmotic potential at full turgor in *Helianthus annuus* plants grown under well-watered (grey circles; $n = 3$) and water-limited condition (black circles; $n = 3$). Dashed lines indicate the mean leaf turgor loss points of plants grown under well-watered (grey line) and water-limited condition (black line)

under high VPD (Figure 5d). Additionally, Ψ_{leaf} was not observed to fall below the threshold water potentials to cause cavitation for any of the three individuals (Figure 5b).

When sunflower plants grown under water-limited conditions were exposed to high VPD, a faster stomatal closure took place than in plants grown under well-watered conditions (compare g_s 10 min after the VPD transitions in Figures 5c and 6c), possibly due to a narrower difference between initial Ψ_{leaf} and Ψ_{tlp} (0.41 ± 0.01 MPa in well-watered plants against 0.34 ± 0.04 MPa in water-limited plants). This resulted in a considerably lower peak of E than in plants grown under water-limited conditions (compare Figures 5 and 6). A consistent approximately 40% loss of apparent K_{plant} was observed under high VPD compared with low VPD within all three individuals (Figure 6d), yet Ψ_{leaf} was not observed to fall below the threshold causing incipient cavitation (Figure 6b).

4 | DISCUSSION

Coupling physiological and anatomical data with results from the recently developed OV method (Brodrigg et al., 2016), we demonstrate tight coordination between osmotic adjustment in sunflower plants, induced by soil water-stress, and changes in xylem vulnerability to cavitation. The result of parallel adjustment in these key physiological traits is that water-limited sunflowers are able to extract more water from soils without risking xylem cavitation or leaf damage. Additionally, rapid stomatal responsiveness in sunflower leaves appears to prevent major damage to xylem tissue even when whole plants were subjected to very rapid transitions to very high VPD. Adjustments in xylem vulnerability in response to dry soils, stomatal closure in response to dry atmospheres, and osmotic adjustment to protect photosynthetic systems are proposed as crucial mechanisms allowing survival of sunflower plants under water-limited conditions.

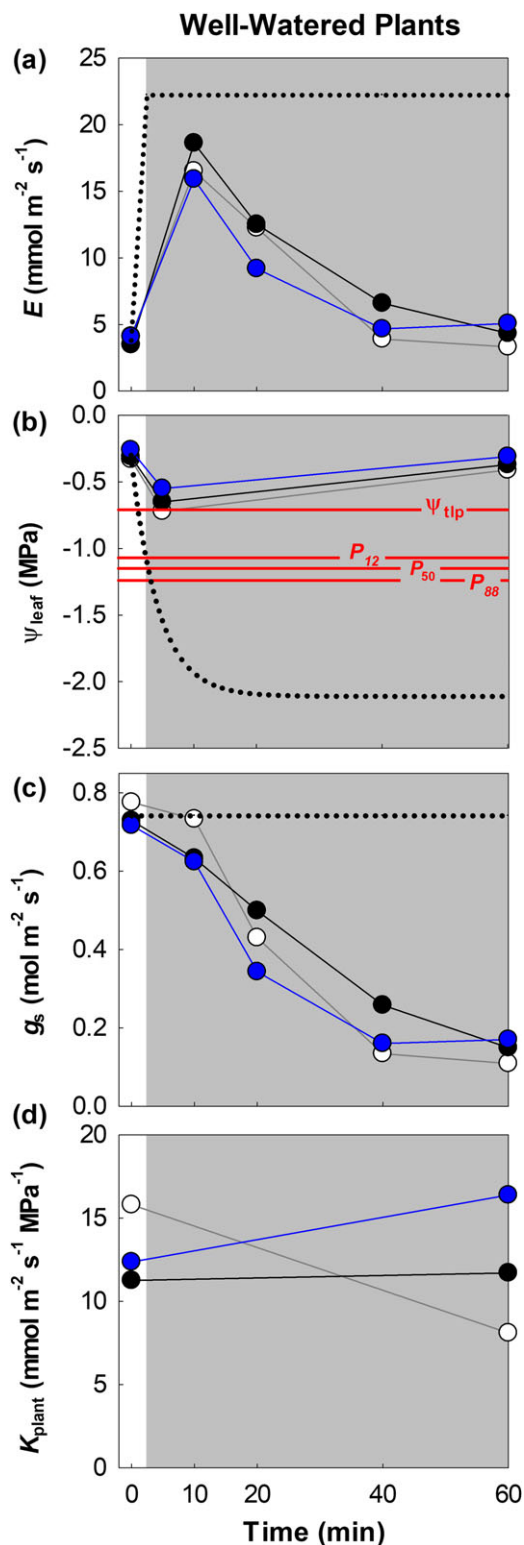


FIGURE 5 (a–c) Dynamic response of transpiration rate (E), leaf water potential (Ψ_{leaf}), stomatal conductance (g_s) and apparent plant hydraulic conductance (K_{plant}) in *Helianthus annuus* plants grown under well-watered conditions, exposed to a step change in vapour pressure deficit (VPD) from approximately 0.75 kPa (white region) to approximately 3.25 kPa (grey region). The different colours indicate individual plants. Dotted lines indicate how these parameters would behave considering no stomatal closure during the VPD transition. Water potentials at turgor loss point (Ψ_{tlp}) and 12%, 50% and 88% cumulative embolism in the leaf midrib (P_{12} , P_{50} and P_{88}) are depicted in (c) [Colour figure can be viewed at wileyonlinelibrary.com]

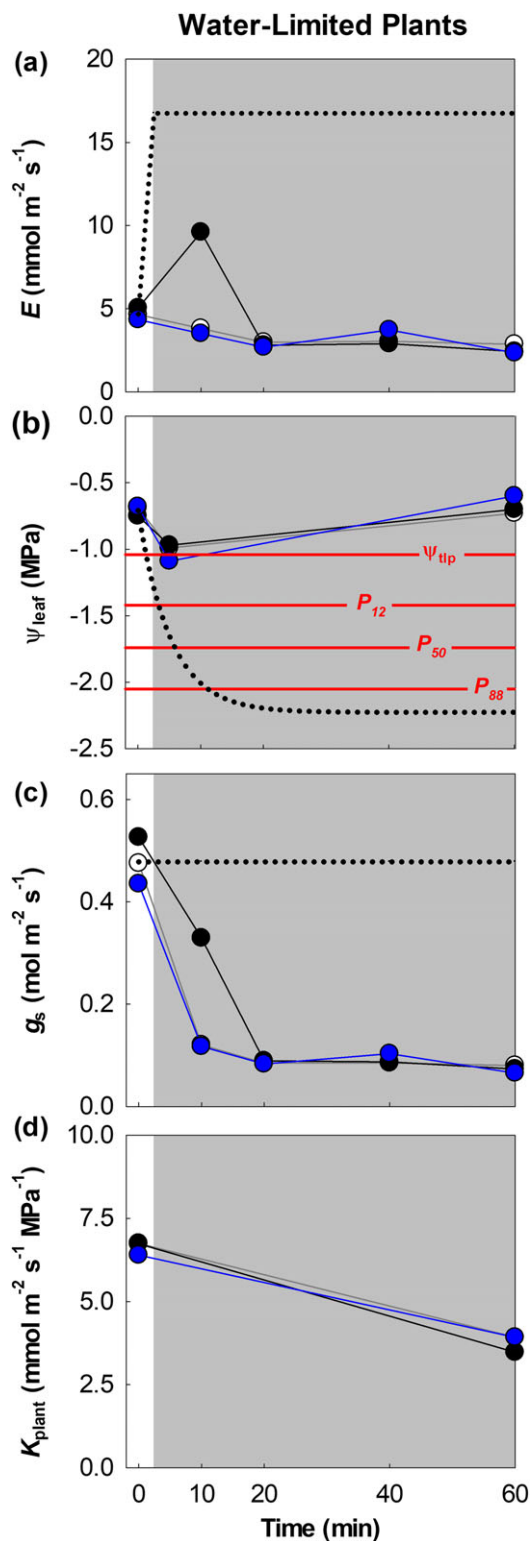


FIGURE 6 (a–d) Dynamic response of transpiration rate (E), leaf water potential (Ψ_{leaf}), stomatal conductance (g_s) and apparent plant hydraulic conductance (K_{plant}) in *Helianthus annuus* plants grown under water-limited conditions exposed to a step change in vapour pressure deficit (VPD) from approximately 0.75 kPa (white region) to approximately 3.25 kPa (grey region). The different colours indicate individual plants. Dotted lines indicate how these parameters would behave considering no stomatal closure during the VPD transition. Water potentials at turgor loss point (Ψ_{tlp}) and 12%, 50% and 88% cumulative embolism in the leaf midrib (P_{12} , P_{50} and P_{88}) are depicted in (c) [Colour figure can be viewed at wileyonlinelibrary.com]

4.1 | Coordinated plasticity in hydraulic and stomatal dynamics enables safer water extraction from drier soils

Sunflower leaves are known to substantially adjust osmotic potential (Ψ_s) when exposed to dry soil (Turner, Begg, & Tonnet, 1978). This was clearly confirmed here. Adjustment of cellular solute potential in water-limited plants provided leaves with the advantage of sustaining gas exchange and photosynthesis as Ψ_{predawn} dropped. Our principle question was to determine how a species that was vulnerable to xylem cavitation could freely adjust Ψ_s , reducing stomatal and photosynthetic sensitivity to water potential, without incurring costs in terms of xylem dysfunction caused by cavitation as Ψ_{leaf} dropped during the day. The answer to this question was revealed in terms of a remarkable degree of plasticity in xylem vulnerability of sunflower leaves. As a result, we found coordinated changes in solute potential, stomatal and photosystem sensitivity to water potential, and xylem vulnerability. This coordinated response enabled sunflower to respond to drier soil by enhancing water extraction capacity while preventing extensive cavitation by closing stomata.

Vulnerability of plant species to xylem cavitation is recognized as a key trait limiting species ability to survive during soil drought (Choat et al., 2012; Skelton et al., 2017), as well as determining species distribution (Blackman, Brodribb, & Jordan, 2012; Larter et al., 2017). Furthermore, as the threshold water potential for air-seeding is thought to exhibit low plasticity in plant species (Choat et al., 2012; Lamy et al., 2014), it is tempting to expect that highly vulnerable species, such as sunflower, would be restricted to wet environments. Contrary to this hypothesis, sunflower plants are commonly found to survive under relatively dry conditions (e.g., Tardieu et al., 1996). Our results provide an explanation for these observations, by demonstrating high plasticity in xylem vulnerability in sunflower that enables plants grown under water-limited conditions to maintain the integrity of their water transport system under conditions that would be lethally damaging in unadjusted plants. For instance, the Ψ_{predawn} of the water-limited treatment 36 hr after watering (i.e., -1.84 MPa; Figure 1) would very quickly exceed the P_{88} (i.e., -1.24 MPa) and even the water potential threshold triggering a decline in F_v/F_m (i.e., -1.63 MPa) if the plants maintained the same xylem vulnerability as plants from the well-watered treatment (Figure 1). However, this Ψ_{predawn} was instead maintained within the P_{50} - P_{88} range of the hydraulically adjusted plants, allowing their survival. Similarly, the water potential 5 min after the VPD transition of the water-limited treatment (i.e., -1.02 MPa) would be very close to the P_{12} (i.e., -1.06 MPa) if plants did not show any hydraulic adjustment (Figure 6).

Our results contrast with previous studies reporting very low levels of within-species variation in P_{50} of stems (Corcuera, Cochard, Gil-Pelegrin, & Notivol, 2011; Plavcová, Hacke, & Sperry, 2011) and leaves (Blackman, Aspinwall, Tissue, & Rymer, 2017; Nolf, Rosani, Ganthaler, Beikircher, & Mayr, 2016). Given that leaves have a shorter lifespan and are usually exposed to greater variations in water potential, it seems likely that they may exhibit a higher degree of plasticity in vulnerability when compared to stems. When considered in the context of relatively low plasticity of stem vulnerability in sunflower

(Stiller & Sperry, 2002; Ahmad et al., 2018), this seems to be the case for this species. Additionally, it is notable that sunflower appears to exhibit a higher degree of vulnerability segmentation than other herbs such as tomato (Skelton et al., 2017). The ecology of segmentation among herbs and woody plants seems to be quite diverse and will be a rich field for future research.

More cavitation-resistant xylem is expected to incur costs in terms of xylem construction, as the development of more negative pressures within the conduits could result in cell collapse if leaf xylem were not sufficiently reinforced to withstand mechanical collapse (Blackman et al., 2010; Hacke, Sperry, Pockman, Davis, & McCulloch, 2001). In this regard, our results demonstrate that reductions in xylem vulnerability in osmotically adjusted plants were also accompanied by thicker cell walls in the xylem conduits of the midrib, and hence higher $(t/b)^3$ (Table 1). This more mechanically reinforced xylem could resist more negative xylem pressures before buckling and becoming non-conductive during water stress (Zhang, Rockwell, Graham, Alexander, & Holbrook, 2016).

As well as producing more robust xylem, we found that the photosynthetic apparatus was more robust to dehydration in plants grown under water-limited conditions. Based upon declines in F_v/F_m , during acute dehydration, we provide compelling evidence that complete hydraulic failure in the midrib precedes drought damage in terms of photosynthetic damage in sunflower (Figure 3), much like previous studies that associate leaf damage with extensive cavitation, ie, starting from P_{88} to P_{95} (Brodribb & Cochard, 2009; Skelton et al., 2017).

As sunflower leaves dehydrate, a conservative sequence of physiological events occurs: loss of bulk leaf turgor, xylem cavitation, and ultimately tissue injury (Figure 3). Similar patterns have been previously discussed (Brodribb, Holbrook, Edwards, & Gutiérrez, 2003; Maréchaux, Bartlett, Iribar, Sack, & Chave, 2017; Nolf et al., 2016), and here, we provide further insights on (a) how this sequence is functionally important to prevent drought-induced xylem cavitation and consequent major losses of hydraulic conductance, and on (b) physiological mechanisms in angiosperms that enable plasticity in stomatal closure to avoid drought-induced damage, (c) and most importantly, how changing the threshold for one of these physiological mechanisms in sunflower results in a parallel shift in all mechanisms.

Stomatal closure is usually associated with increases in VPD in angiosperm species. In this regard, our VPD data (Figures 5 and 6) demonstrate that as soon as VPD increases, Ψ_{leaf} transiently decreases, falling close or below Ψ_{tip} within minutes, and consequently inducing stomatal closure. Only fast and efficient stomatal closure prevents further decreases in Ψ_{leaf} , which could otherwise result in extensive xylem cavitation. However, declines in apparent K_{plant} were observed in one well-watered individual and in the three water-limited individuals. A possible explanation is that such declines resulted from modifications in the outside-xylem pathway (Cuneo, Knipfer, Brodersen, & McElrone, 2016; Scoffoni et al., 2017), because Ψ_{leaf} was not observed to fall close to the threshold causing incipient cavitation under high VPD (Figures 5b and 6b). Without stomatal closure under high VPD (dotted lines in Figures 5b and 6b), 88% of xylem conduits in the leaf midrib would be cavitated in less than 10 min after a switch from low to high VPD in sunflower plants (Figures 5 and 6).

This result per se strongly pinpoints stomatal closure as an exceedingly important mechanism by which herbs prevent hydraulic failure under high VPD, adding to the well-known importance of stomatal closure to prevent cavitation during soil water stress in woody plants (Brodribb, McAdam, & Murphy, 2017; Martin-StPaul et al., 2017).

5 | CONCLUSION

A coordinated plasticity in xylem and stomatal sensitivity to water deficit enables water-limited sunflowers to safely extract water from the soil, while protecting leaf xylem against embolism. This high plasticity in sunflower xylem contrasts with data from woody plants and may suggest an alternative strategy in herbaceous species.

ACKNOWLEDGMENTS

The authors gratefully acknowledge funding support from the Australian Research Council (grants DE140100946 [S. A. M. M.] and DP140100666 [T. J. B.]) and the Brazilian government via FAPEMIG (visiting scholarship no. BDS-00404-15 [A. A. C.]). CSIRO Hobart is acknowledged for the stem psychrometers used during the experiments, and the dear Dr. Madeline Carins Murphy is acknowledged for helping collect data.

ORCID

Amanda A. Cardoso  <http://orcid.org/0000-0001-7078-6246>

Timothy J. Brodribb  <http://orcid.org/0000-0002-4964-6107>

Scott A.M. McAdam  <http://orcid.org/0000-0002-9625-6750>

REFERENCES

- Ahmad, H. B., Lens, F., Capdeville, G., Burlett, R., Lamarque, L. J., & Delzon, S. (2018). Intraspecific variation in embolism resistance and stem anatomy across four sunflower (*Helianthus annuus* L.) accessions. *Physiol Plantarum*, *163*, 59–72.
- Anderegg, W. R. L. (2014). Spatial and temporal variation in plant hydraulic traits and their relevance for climate change impacts on vegetation. *New Phytologist*, *205*, 1008–1014.
- Blackman, C. J., Aspinwall, M. J., Tissue, D. T., & Rymer, P. D. (2017). Genetic adaptation and phenotypic plasticity contribute to greater leaf hydraulic tolerance in response to drought in warmer climates. *Tree Physiology*, *37*, 583–592.
- Blackman, C. J., Brodribb, T. J., & Jordan, G. J. (2010). Leaf hydraulic vulnerability is related to conduit dimensions and drought resistance across a diverse range of woody angiosperms. *New Phytologist*, *188*, 1113–1123.
- Blackman, C. J., Brodribb, T. J., & Jordan, G. J. (2012). Leaf hydraulic vulnerability influences species' bioclimatic limits in a diverse group of woody angiosperms. *Oecologia*, *168*, 1–10.
- Brodribb, T. J., & Cochard, H. (2009). Hydraulic failure defines the recovery and point of death in water-stressed conifers. *Plant Physiology*, *149*, 575–584.
- Brodribb, T. J., Feild, T. S., & Jordan, G. J. (2007). Leaf maximum photosynthetic rate and venation are linked by hydraulics. *Plant Physiology*, *144*, 1890–1898.
- Brodribb, T. J., & Holbrook, N. M. (2003). Stomatal closure during leaf dehydration, correlation with other leaf physiological traits. *Plant Physiology*, *132*, 2166–2173.
- Brodribb, T. J., & Holbrook, N. M. (2005). Water stress deforms tracheids peripheral to the leaf vein of a tropical conifer. *Plant Physiology*, *137*, 1139–1146.
- Brodribb, T. J., & Holbrook, N. M. (2006). Declining hydraulic efficiency as transpiring leaves desiccate: Two types of response. *Plant, Cell & Environment*, *29*, 2205–2215.
- Brodribb, T. J., Holbrook, N. M., Edwards, E. J., & Gutiérrez, M. V. (2003). Relations between stomatal closure, leaf turgor and xylem vulnerability in eight tropical dry forest trees. *Plant, Cell & Environment*, *23*, 443–450.
- Brodribb, T. J., & McAdam, S. A. M. (2017). Evolution of the stomatal regulation of plant water content. *Plant Physiology*, *174*, 639–649.
- Brodribb, T. J., McAdam, S. A. M., & Murphy, M. R. C. (2017). Xylem and stomata, coordinated through time and space. *Plant, Cell & Environment*, *40*, 872–880.
- Brodribb, T. J., Skelton, R. P., McAdam, S. A. M., Bienaimé, D., Lucani, C. J., & Marmottant, P. (2016). Visual quantification of embolism reveals leaf vulnerability to hydraulic failure. *New Phytologist*, *209*, 1403–1409.
- Buckley, T. N. (2005). The control of stomata by water balance. *New Phytologist*, *168*, 275–292.
- Choat, B., Jansen, S., Brodribb, T. J., Cochard, H., Delzon, S., Bhaskar, R., ... Zanne, A. E. (2012). Global convergence in the vulnerability of forests to drought. *Nature*, *7426*, 752–755.
- Cochard, H., Coll, L., Le Roux, X., & Améglio, T. (2002). Unraveling the effects of plant hydraulics on stomatal closure during water stress in walnut. *Plant Physiology*, *128*, 282–290.
- Corcuera, L., Cochard, H., Gil-Pelegrin, E., & Notivol, E. (2011). Phenotypic plasticity in mesic populations of *Pinus pinaster* improves resistance to xylem embolism (P_{50}) under severe drought. *Trees*, *25*, 1033–1042.
- Cuneo, I. F., Knipfer, T., Brodersen, C. R., & McElrone, A. J. (2016). Mechanical failure of fine root cortical cells initiates plant hydraulic decline during drought. *Plant Physiology*, *172*, 1669–1678.
- Dixon, H. H., & Joly, J. (1895). The path of the transpiration current. *Annals of Botany*, *9*, 416–419.
- Gleason, S. M., Wiggans, D. R., Bliss, C. A., Young, J. S., Cooper, M., Willi, K. R., & Comas, L. H. (2017). Embolized stems recover overnight in *Zea mays*: The role of soil water, root pressure, and nighttime transpiration. *Frontiers in Plant Science*, *8*, 1–11.
- Guadagno, C. R., Ewers, B. E., Speckman, H. N., Aston, T. L., Huhn, B. J., DeVore, S. B., ... Weinig, C. (2017). Dead or alive? Using membrane failure and chlorophyll a fluorescence to predict plant mortality from drought. *Plant Physiology*. <https://doi.org/10.1104/pp.16.00581>
- Hacke, U. G., Sperry, J. S., Pockman, W. T., Davis, S. D., & McCulloch, K. A. (2001). Trends in wood density and structure are linked to the prevention of xylem implosion by negative pressure. *Oecologia*, *126*, 457–461.
- Hacke, U. G., Sperry, J. S., Wheeler, J. K., & Castro, L. (2006). Scaling of angiosperm xylem structure with safety and efficiency. *Tree Physiology*, *26*, 689–701.
- Kolb, K. J., & Sperry, J. S. (1999). Differences in drought adaptation between subspecies of Sagebrush (*Artemisia tridentata*). *Ecology*, *80*, 2373–2384.
- Korson, L., Drost-Hansen, W., & Millero, F. J. (1969). Viscosity of water at various temperatures. *The Journal of Physical Chemistry A*, *73*, 34–39.
- Lamy, J.-B., Delzon, S., Bouche, P. S., Alia, R., Vendramin, G. G., Cochard, H., & Plomion, C. (2014). Limited genetic variability and phenotypic plasticity detected for cavitation resistance in a Mediterranean pine. *New Phytologist*, *201*, 874–886.
- Larter, M., Brodribb, T., Pfautsch, S., Burlett, R., Cochard, H., & Delzon, S. (2015). Extreme aridity pushes trees to their physical limits. *Plant Physiology*, *168*, 804–807.
- Larter, M., Pfautsch, S., Domec, J. C., Trueba, S., Nagalingum, N., & Delzon, S. (2017). Aridity drove the evolution of extreme embolism resistance and the radiation of conifer genus *Callitris*. *New Phytologist*, *215*, 97–112.
- Lens, F., Picon-Cochard, C., Delmas, C. E., Signarbieux, C., Buttler, A., Cochard, H., ... Delzon, S. (2016). Herbaceous angiosperms are not more vulnerable to drought-induced embolism than angiosperm trees. *Plant Physiology*, *172*, 661–667.

- Li, Y., Sperry, J. S., & Shao, M. (2009). Hydraulic conductance and vulnerability to cavitation in corn (*Zea mays* L.) hybrids of differing drought resistance. *Environmental and Experimental Botany*, *66*, 341–346.
- Maréchaux, I., Bartlett, M. K., Iribar, A., Sack, L., & Chave, J. (2017). Stronger seasonal adjustment in leaf turgor loss point in lianas than trees in an Amazonian forest. *Biology Letters*, *13*, 20160819.
- Martin-StPaul, N., Delzon, S., & Cochard, H. (2017). Plant resistance to drought depends on timely stomatal closure. *Ecology Letters*, *20*, 1437–1447. <https://doi.org/10.1111/ele.12851>
- Nolf, M., Rosani, A., Ganthaler, A., Beikircher, B., & Mayr, S. (2016). Herb hydraulics: Inter- and intraspecific variation in three *Ranunculus* species. *Plant Physiology*, *170*, 2085–2094.
- Oren, R., Sperry, J. S., Katul, G., Pataki, D. E., Ewers, B. E., Phillips, N., & Schafer, K. V. R. (1999). Survey and synthesis of intra- and inter-specific variation in stomatal sensitivity to vapor pressure deficit. *Plant, Cell & Environment*, *22*, 1515–1526.
- Plavcová, L., Hacke, U. G., & Sperry, J. S. (2011). Linking irradiance-induced changes in pit membrane ultrastructure with xylem vulnerability to cavitation. *Plant, Cell & Environment*, *34*, 501–513.
- Reich, P. B. (2014). The world-wide 'fast-slow' plant economics spectrum: A traits manifesto. *Journal of Ecology*, *102*, 275–301.
- Sack, L., & Holbrook, N. M. (2006). Leaf hydraulics. *Annual Review of Plant Biology*, *57*, 361–381.
- Sack, L., Melcher, P. J., Zwieniecki, M. A., & Holbrook, N. M. (2002). The hydraulic conductance of the angiosperm leaf lamina: A comparison of three measurement methods. *Journal of Experimental Botany*, *53*, 2177–2184.
- Saha, S., Holbrook, N. M., Montti, L., Goldstein, G., & Cardinot, G. K. (2009). Water relations of *Chusquea ramosissima* and *Merostachys clausenii* in Iguazu national park, Argentina. *Plant Physiology*, *149*, 1992–1999.
- Scoffoni, C., Albuquerque, C., Brodersen, C., Townes, S. V., John, G. P., ... Sack, L. (2017). Outside-xylem vulnerability, not xylem embolism, controls leaf hydraulic decline during dehydration. *Plant Physiology*, *173*, 1197–1210.
- Skelton, R. P., Brodribb, T. J., & Choat, B. (2017). Casting light on xylem vulnerability in an herbaceous species reveals a lack of segmentation. *New Phytologist*, *214*, 561–569.
- Sperry, J. S. (2000). Hydraulic constraints on gas exchange. *Agricultural and Forest Meteorology*, *104*, 13–23.
- Sperry, J. S., & Tyree, M. T. (1988). Mechanism of water stress induced xylem embolism. *Plant Physiology*, *88*, 581–587.
- Stiller, V., & Sperry, J. S. (2002). Cavitation fatigue and its reversal in sunflower (*Helianthus annuus* L.). *Journal of Experimental Botany*, *53*, 1155–1161.
- Tardieu, F., Lafarge, T., & Simonneau, T. H. (1996). Stomatal control by fed or endogenous xylem ABA in sunflower: Interpretation of correlations between leaf water potential and stomatal conductance in anisohydric species. *Plant, Cell & Environment*, *19*, 75–84.
- Turner, N. C., Begg, J. E., & Tonnet, M. L. (1978). Osmotic adjustment of sorghum and sunflower crops in response to water deficits and its influence on the water potential at which stomata close. *Functional Plant Biology*, *5*, 597–608.
- Turner, N. C., & Jones, H. G. (1980). Turgor maintenance by osmotic adjustment: A review and evaluation. In N. C. Turner, & P. J. Kramer (Eds.), *Adaptation of Plants to Water and High Temperature Stress* (pp. 87–103). New York: Wiley Interscience.
- Tyree, M. T., & Hammel, H. T. (1972). The measurement of the turgor pressure and the water relations of plants by the pressure-bomb technique. *Journal of Experimental Botany*, *23*, 267–282.
- Tyree, M. T., & Sperry, J. S. (1989). Vulnerability of xylem to cavitation and embolism. *Annual Review of Plant Physiology and Plant Molecular Biology*, *40*, 19–38.
- Zhang, Y. J., Rockwell, F. E., Graham, A. C., Alexander, T., & Holbrook, N. M. (2016). Reversible leaf xylem collapse: A potential "circuit breaker" against cavitation. *Plant Physiology*, *172*, 2261–2274.

How to cite this article: Cardoso AA, Brodribb TJ, Lucani CJ, DaMatta FM, McAdam SAM. Coordinated plasticity maintains hydraulic safety in sunflower leaves. *Plant Cell Environ.* 2018;41:2567–2576. <https://doi.org/10.1111/pce.13335>